

NanoScience and Technology

Enrico Gnecco
Ernst Meyer *Editors*

Fundamentals of Friction and Wear on the Nanoscale

Second Edition

 Springer

NanoScience and Technology

Series editors

Phaedon Avouris, Yorktown Heights, USA

Bharat Bhushan, Columbus, USA

Dieter Bimberg, Berlin, Germany

Klaus von Klitzing, Stuttgart, Germany

Hiroyuki Sakaki, Tokyo, Japan

Roland Wiesendanger, Hamburg, Germany

The series NanoScience and Technology is focused on the fascinating nano-world, mesoscopic physics, analysis with atomic resolution, nano and quantum-effect devices, nanomechanics and atomic-scale processes. All the basic aspects and technology-oriented developments in this emerging discipline are covered by comprehensive and timely books. The series constitutes a survey of the relevant special topics, which are presented by leading experts in the field. These books will appeal to researchers, engineers, and advanced students.

More information about this series at <http://www.springer.com/series/3705>

Enrico Gnecco · Ernst Meyer
Editors

Fundamentals of Friction and Wear on the Nanoscale

Second Edition

 Springer

Editors

Enrico Gnecco
Instituto Madrileño de Estudios Avanzados
en Nanociencia
Madrid
Spain

Ernst Meyer
Department of Physics
University of Basel
Basel
Switzerland

This is a second edition. ISBN 1st ed.: 978-3-540-36806-9

ISSN 1434-4904

ISSN 2197-7127 (electronic)

ISBN 978-3-319-10559-8

ISBN 978-3-319-10560-4 (eBook)

DOI 10.1007/978-3-319-10560-4

Library of Congress Control Number: 2014952447

Springer Cham Heidelberg New York Dordrecht London

© Springer International Publishing Switzerland 2015

This work is subject to copyright. All rights are reserved by the Publisher, whether the whole or part of the material is concerned, specifically the rights of translation, reprinting, reuse of illustrations, recitation, broadcasting, reproduction on microfilms or in any other physical way, and transmission or information storage and retrieval, electronic adaptation, computer software, or by similar or dissimilar methodology now known or hereafter developed. Exempted from this legal reservation are brief excerpts in connection with reviews or scholarly analysis or material supplied specifically for the purpose of being entered and executed on a computer system, for exclusive use by the purchaser of the work. Duplication of this publication or parts thereof is permitted only under the provisions of the Copyright Law of the Publisher's location, in its current version, and permission for use must always be obtained from Springer. Permissions for use may be obtained through RightsLink at the Copyright Clearance Center. Violations are liable to prosecution under the respective Copyright Law.

The use of general descriptive names, registered names, trademarks, service marks, etc. in this publication does not imply, even in the absence of a specific statement, that such names are exempt from the relevant protective laws and regulations and therefore free for general use.

While the advice and information in this book are believed to be true and accurate at the date of publication, neither the authors nor the editors nor the publisher can accept any legal responsibility for any errors or omissions that may be made. The publisher makes no warranty, express or implied, with respect to the material contained herein.

Printed on acid-free paper

Springer is part of Springer Science+Business Media (www.springer.com)

Preface

The second edition of “Fundamentals of Friction and Wear on the Nanoscale” has been motivated by the significant progress made by nano tribology in the last seven years. New chapters on triboluminescence, friction in liquids, nonlinear mechanisms of friction, fractal surfaces, multiscale modeling of contacts, capillary condensation, nano manipulation in SEM, colloidal systems, graphene, nanowear of polymers, Casimir forces, and cell motility have been added. Other key chapters, such as those on atomic-scale friction in ultra-high vacuum and nano manipulation have been completely revised. On the other side, we have omitted some chapters dealing with side aspects of nano tribology which did not undergo significant changes in the last few years. We hope that this new edition will attract the interest of a broad readership of scientists and engineers, and stimulate new experiments and theoretical models in this exciting multidisciplinary research field.

Madrid
Basel

Enrico Gnecco
Ernst Meyer

Contents

Part I Experimental Techniques

1	Friction Force Microscopy	3
	Roland Bennewitz	
1.1	Introduction	3
1.2	Instrumentation	4
	1.2.1 Force Sensors	4
	1.2.2 Control Over the Contact	7
1.3	Measurement Procedures	9
	1.3.1 Friction as a Function of Load	9
	1.3.2 Friction as a Function of Material	11
	1.3.3 Friction Effects in Normal Force Measurements	11
	1.3.4 Fluctuations in Friction Force Microscopy	11
	1.3.5 Friction as a Function of Temperature	12
	1.3.6 Dynamic Lateral Force Measurements	12
1.4	Outlook	14
	References	14
2	Surface Forces Apparatus in Nanotribology	17
	Carlos Drummond and Philippe Richetti	
2.1	Introduction	17
2.2	Surface Forces Apparatus Technique: Generalities	18
2.3	Surface Forces Apparatus Nanotribometer	20
	2.3.1 Experimental Setup	21
	2.3.2 Local Structural Information: Combination of the SFA with Other Techniques	25
	2.3.3 Beyond Mica: Alternative Substrates	27
2.4	Case Study: Weakly Adhesive Surfaces Under Shear	29
	References	32

3	Nanoscale Friction and Ultrasonics	35
	Maria Teresa Cuberes	
3.1	Introduction	35
3.2	Normal Ultrasonic Vibration at Nanocontacts	37
3.3	Shear Ultrasonic Vibration at Nanocontacts	43
3.4	Reduction of Friction by Ultrasonic Vibration	44
3.5	Adhesion Hysteresis at Ultrasonic Frequencies	48
	References.	53
4	Triboluminescence	57
	Roman Nevshupa and Kenichi Hiratsuka	
4.1	Introduction and Brief Historical Survey	57
4.2	Basic Processes and Activation Mechanisms	59
4.3	Experimental Techniques for Studying Triboluminescence	62
4.4	Characteristics of the TL	65
4.4.1	Spatial Distribution of the TL at a Tribological Contact	65
4.4.2	Effect of the Ambient Gas and the Material of the Counterbodies on Spectral Characteristics and Intensity Distribution of the TL	67
4.4.3	Effect of Friction Type and Humidity on the TL and Triboelectrification of Polymers.	70
4.4.4	Behaviour of the TL on Different Time Scales	72
4.5	Modelling Approach	73
	References.	75
5	The Quartz Crystal Microbalance as a Nanotribology Technique	79
	Lorenzo Bruschi and Giampaolo Mistura	
5.1	Introduction	79
5.2	The Acoustics of Quartz Crystal	80
5.3	QCM Driving Circuits.	83
5.4	Quality of the Surface Electrodes	86
5.5	UHV Apparatus	88
	References.	90
 Part II Atomic-Scale Friction		
6	Atomic-Scale Friction Measurements in Ultra-High Vacuum.	95
	Sabine Maier, Enrico Gnecco and Ernst Meyer	
6.1	Introduction	95
6.2	The Prandtl-Tomlinson Model	97

6.2.1	One-dimensional Prandtl-Tomlinson Model	97
6.2.2	Extensions of the Prandtl-Tomlinson Model	100
6.3	Experimental Observations of Atomic Stick-slip	101
6.3.1	Load Dependence: From Smooth Sliding and Stick-slip to Wear	102
6.3.2	The Slip	104
6.3.3	Thermal Effects and Velocity Dependence	104
6.3.4	Maximal Lateral Force	106
6.3.5	Multiple Slips	106
6.4	Atomic-Scale Friction Beyond Flat Terraces	107
6.4.1	Atomic-Scale Friction at Step Edges	107
6.4.2	Atomic-Scale Friction on Ordered Superstructures and Reconstructions	108
6.5	Anisotropy Effects	109
6.6	Mechanical Properties of Molecular Chains	110
6.7	Conclusions	112
	References	112
7	Stochastic Modeling and Rate Theory of Atomic Friction	115
	Mykhaylo Evstigneev, Juan J. Mazo and Peter Reimann	
7.1	Introduction	115
7.2	Langevin Modeling	117
7.2.1	Langevin Equation	117
7.2.2	Parameter Values	120
7.2.3	Regimes of Motion	121
7.2.4	Some Generalizations of the Standard PT Model	123
7.2.5	Friction Force-velocity Relations	124
7.3	Rate Theory	126
7.3.1	Rate Equation	126
7.3.2	Validity Conditions	128
7.3.3	Parameterization	128
7.3.4	Types of the Stick-slip Motion	130
7.3.5	Force-velocity Relations	131
7.3.6	Force Probability Distribution	133
7.4	Concluding Remarks	134
	References	135
8	Experimental Observations of Superlubricity and Thermolubricity	139
	Martin Dienwiebel and Joost W.M. Frenken	
8.1	Introduction	139
8.1.1	The Transition to Frictionless Sliding in the One-Dimensional Case	140

8.1.2	Superlubricity	141
8.1.3	In Search for Superlubricity	141
8.2	Atomic-Scale Observation of Superlubricity	142
8.2.1	Commensurability-Dependent Superlubricity Between Finite Graphite Surfaces	142
8.2.2	The Role of the Normal Force	147
8.3	The Role of Temperature	149
8.3.1	Weak Thermal Effects	149
8.3.2	Strong Thermal Effects: Thermolubricity	150
8.4	Other Manifestations of Superlubricity and Thermolubricity	152
8.4.1	Lubrication by Graphite and Other Lamellar Solids	152
8.4.2	Lubrication by Diamond-Like Carbon and Related Coatings	153
8.4.3	Lubrication by Fullerenes and Carbon Nanotubes	153
8.5	Concluding Remarks	154
	References	155
9	Friction and Wear of Mineral Surfaces in Liquid Environments	157
	Carlos M. Pina, Carlos Pimentel and E. Gnecco	
9.1	Introduction	157
9.2	Structural Studies of Mineral Surfaces Using Lateral Force Microscopy	159
9.3	Obtaining Chemical Information of Surfaces from Frictional Forces	162
9.4	Wear and Nanomanipulation of Mineral Surfaces and Overgrowths	164
9.5	Organic Molecules on Mineral Surfaces	168
9.6	Conclusions and Outlook	171
	References	172
10	Nanotribology: Nonlinear Mechanisms of Friction	175
	N. Manini, Oleg M. Braun and A. Vanossi	
10.1	Introduction	175
10.2	The Prandtl-Tomlinson Model	177
10.3	The Frenkel-Kontorova Model	181
10.3.1	Extensions of the Frenkel-Kontorova Model	187
10.4	Molecular Dynamics Simulations	191
10.4.1	Thermostats and Joule Heat	193
10.4.2	Size- and Time-scale Issues	193
10.4.3	Multiscale Models	195
10.4.4	Selected Results of MD Simulations	195

10.5 Earthquake-Like Models 198

10.6 Conclusions 201

References. 203

11 Theoretical Studies of Superlubricity 209

Martin H. Müser

11.1 Introduction 209

11.2 Theory 211

 11.2.1 Definition of Superlubricity 211

 11.2.2 Cancellation of Lateral Forces. Symmetry
 Considerations 212

 11.2.3 Role of Instabilities in Simple Models. 219

 11.2.4 Effect of Temperature 220

 11.2.5 Damping in the Superlubric Regime 221

 11.2.6 Long-Range Elastic Deformations. 221

 11.2.7 Self-affine Rough Surfaces. 224

11.3 Simulations 225

 11.3.1 Generic Models 225

 11.3.2 Layered Materials 227

 11.3.3 Metal on Metal Contacts 228

 11.3.4 Hydrogen-Terminated Surfaces. 229

11.4 Conclusions 230

References. 231

Part III Multiscale Friction

12 On the Fractal Dimension of Rough Surfaces. 235

Bo Persson

12.1 Introduction 235

12.2 Power Spectrum: Definition 236

12.3 Power Spectra: Some Examples 237

12.4 Simulation of Rough Surfaces: A Simple Erosion Process 241

12.5 Discussion and Summary. 243

References. 247

**13 Contact Mechanics, Friction and Adhesion with Application
to Quasicrystals 249**

Bo Persson, Giuseppe Carbone, Vladimir N. Samoilov,
Ion M. Sivebaek, Ugo Tartaglino, Aleksandr I. Volokitin
and Chunyan Yang

13.1 Introduction 249

13.2 Sliding Friction—Role of Elasticity. 251

13.3	Application to Quasicrystals	252
13.4	Surface Roughness	254
13.4.1	Surface Roughness Power Spectra: Definition and General Properties.	256
13.4.2	Surface Roughness Power Spectra: Experimental Results.	260
13.5	Contact Mechanics	264
13.6	Adhesion	271
13.6.1	Adhesion Between Rough Surfaces	272
13.6.2	The Adhesion Paradox	280
13.6.3	The Role of Liquids on Adhesion Between Rough Solid Surfaces	281
13.7	Summary and Outlook.	285
	References.	286
14	MD/FE Multiscale Modeling of Contact	289
	Srinivasa Babu Ramiseti, Guillaume Ancaix and Jean-Francois Molinari	
14.1	Introduction	289
14.2	Modeling Techniques of Contact at Nanoscale	290
14.3	Multiscale Coupling Applied to Contact	292
14.3.1	State of the Art of Multiscale Methods	293
14.3.2	Sliding Friction and Heat Generation.	297
14.4	Finite Temperature Coupling	299
14.4.1	Scale Transfer Operator.	299
14.4.2	Selective Thermostat	300
14.4.3	Heat Balance Equation	301
14.5	Validation and Application.	302
14.5.1	Mechanical Wave Propagation at Finite Temperature.	303
14.5.2	Thermo-Mechanical Wave Propagation	304
14.5.3	Application to Dynamic Contact.	306
14.6	Conclusion.	308
	References.	309
15	Effect of Capillary Condensation on Nanoscale Friction	313
	Rosario Capozza, Itay Barel and Michael Urbakh	
15.1	Introduction	313
15.2	Model	315
15.3	Temperature and Velocity Dependencies of Friction	316
15.4	Effect of Inplane Oscillations	322
15.4.1	Summary.	328
	References.	329

Part IV Nanomanipulation

16 Mechanical Properties of Metallic Nanocontacts	333
Gabino Rubio-Bollinger, Juan J. Riquelme, Sebastian Vieira and Nicolas Agraït	
16.1 Introduction	334
16.2 Experimental Tools	335
16.2.1 The Scanning Tunneling Microscope Supplemented with a Force Sensor	337
16.2.2 The Mechanically Controllable Break-Junction Technique	338
16.3 Electron Transport Through Metallic Nanocontacts	340
16.4 Mechanical Properties of Metallic Nanocontacts	342
16.4.1 Fabrication of Metallic Nanocontacts	342
16.4.2 Elasticity and Fracture of Metallic Nanocontacts	344
16.4.3 The Shape of Metallic Nanocontacts	345
16.4.4 Inelastic Scattering by Phonons in Nanocontacts	347
16.5 Suspended Chains of Single Gold Atoms	348
16.5.1 Fabrication of Chains of Atoms Using Local Probes	348
16.5.2 Mechanical Processes During Formation of Atomic Chains	350
16.5.3 Phonons in Atomic Chains	353
16.6 Metallic Adhesion in Atomic-Sized Tunneling Junctions	357
References	359
17 Nanotribological Studies by Nanoparticle Manipulation	363
Dirk Dietzel, Udo D. Schwarz and André Schirmeisen	
17.1 Nanoparticle Manipulation: An Alternative Route to Nanotribology	363
17.2 Friction Measurements by Nanoparticle Manipulation: Experimental Approach	366
17.2.1 Dynamic AFM Techniques for Nanoparticle Manipulation	366
17.2.2 Contact Mode AFM Techniques for Nanoparticle Manipulation	368
17.2.3 Identifying Static Friction in Nanoparticle Manipulation Experiments	375
17.2.4 Comparison of Manipulation Strategies	378
17.3 Nanoparticles for Manipulation Experiments	378
17.4 Friction of Extended Nanocontacts: Theoretical Concepts	381
17.5 Frictional Duality of Sliding Nanoparticles	385

17.5.1	Contact Area Dependence of Friction Analyzed by Nanoparticle Manipulation	385
17.5.2	The Role of Interface Contaminations: Theoretical Calculations.	388
17.6	Conclusion and Outlook	390
	References.	391
18	Tribological Aspects of In Situ Manipulation of Nanostructures Inside Scanning Electron Microscope.	395
	Boris Polyakov, Leonid Dorogin, Sergei Vlassov, Ilmar Kink and Rünno Lõhmus	
18.1	Introduction	395
18.2	Section I: Instrumentation	397
18.2.1	Nanomanipulators	397
18.2.2	Force Measurements	398
18.3	Section II: Manipulation of Nanoparticles	401
18.3.1	Contact Area	402
18.3.2	Manipulation of Polyhedron-Like Nanoparticles	402
18.3.3	Manipulation of Silver Nanoballs and Nanodumbbells.	404
18.4	Section III: Manipulation of Nanowires	406
18.4.1	Elastic Beam Theory Employed for Tribomechanical Studies of Nanowires	407
18.4.2	Nanowire Loaded at One End	411
18.4.3	Nanowire Pushed in the Midpoint: Kinetic Friction.	417
18.4.4	Redistributed Static Friction of a Bent Nanowire Relaxed After Manipulation	419
18.4.5	Specific Problems of Manipulations Inside SEM	423
18.5	Outlook	423
	References.	424
19	Driven Colloidal Monolayers: Static and Dynamic Friction.	427
	Andrea Vanossi, Nicola Manini and Erio Tosatti	
19.1	Introduction	427
19.2	Sliding of a Colloid Monolayer on Laser-Created Periodic Potentials.	429
19.3	Molecular Dynamics Simulation Model	430
19.4	The Simulation Protocol	434
19.5	Simulation Results	436
19.5.1	Force-Velocity Characteristics	436
19.5.2	Aubry-Like Pinning-Unpinning Transition	437
19.5.3	Soliton-Antisoliton Asymmetry.	437
19.5.4	The Sliding State	438
19.5.5	Phase-Diagram Evolution with Sliding.	440

19.6	Friction of Colloid Sliding on the Optical Lattice	441
19.7	Summary and Discussion	443
	References	449
Part V Layered Materials, Polymers		
20	Micro- and Nanotribology of Graphene	453
	Martin Dienwiebel and Roland Bennewitz	
20.1	Introduction	453
20.2	Friction Force Microscopy of Graphene	454
20.3	Graphene Versus Graphite	455
20.4	Atomic-Scale Friction of Graphene	455
20.5	Atomistic Simulations of Graphene Tribology	457
20.6	Friction and Wear of Graphene at the Microscale	458
20.7	Summary	460
	References	460
21	Superlubricity in Layered Nanostructures	463
	Seymur Cahangirov and Salim Ciraci	
21.1	Introduction	463
	21.1.1 Dissipation Phenomena	464
	21.1.2 Adiabatic Versus Sudden Processes	464
	21.1.3 Prandtl-Tomlinson Model	465
	21.1.4 Motivation	468
21.2	Superlubricity Between Two Layers of Graphene Derivatives and Transition Metal Dichalcogenides	469
	21.2.1 Methods	470
	21.2.2 Critical Curvature	470
	21.2.3 Intrinsic Stiffness	474
	21.2.4 Frictional Figure of Merit	475
	21.2.5 Stick-slip in Silicane: A Counter Example	476
21.3	Superlubricity Between Graphene Coated Metal Substrates	477
	21.3.1 Model and the Atomic Structure	478
	21.3.2 Adhesion Hysteresis	479
	21.3.3 Trends in Multilayers	481
	21.3.4 Analysis of Charge Density	483
21.4	Discussions and Conclusions	485
	References	486
22	Nanoscale Friction of Self-assembled Monolayers	489
	Karine Mougou and Haidara Hamidou	
22.1	Homogeneous Organic Molecular Films	490
	22.1.1 Influence of Chain Length and Structure	493

22.1.2	Influence of Terminal Group	495
22.1.3	Effect of Humidity and Temperature	496
22.1.4	Influence of Sliding Velocity	498
22.1.5	Conclusion.	499
22.2	Molecular Heterogeneous Thin Films	500
22.2.1	Influence of Topology	500
22.2.2	Influence of Sliding Velocity	509
22.3	Wear of SAMs.	511
22.4	Conclusion.	512
	References.	513

Part VI Nanowear

23	From Nano and Microcontacts to Wear of Materials	517
	Rogério Colaço	
23.1	Introduction	517
23.2	The Nature of Solid Surfaces	519
23.2.1	Surface Constitution	519
23.2.2	Surface Topography	520
23.2.3	Topographic Mechanisms of Wear	522
23.3	Wear Theories	524
23.3.1	Classical Wear Theories.	524
23.3.2	Atomic Wear Theories.	527
23.4	Wear Experiments at Submicrometric Scales Using the AFM	530
23.5	Indentation Size Effect	535
23.6	Conclusions	538
	References.	539
24	Nanowear of Polymers	545
	Mario D'Acunto, Franco Dinelli and Pasqualantonio Pingue	
24.1	Introduction	546
24.2	Wear Tests at the Nanoscale in Polymer Films to Assess Material Properties	553
24.2.1	Schallamach Waves and Ripples.	554
24.2.2	Multiple Line Scratch Test.	555
24.2.3	Amorphousness and Crystallinity	557
24.2.4	Plasma Treatment	559
24.2.5	Presence of Solvent.	560
24.2.6	Temperature Dependence.	561
24.2.7	Composites	562
24.2.8	Boundary Conditions.	566

24.3 Exploiting the Nanowear of Polymers for Lithographic Applications. 567

24.4 Characterization of Meso- and Nanoscale Wear of Polymers in Biomedical Applications 579

 24.4.1 Role of Wear Rates for Biodegradable Polymers. 580

 24.4.2 Severe Wear Regime in Biomaterials: Wear of UHMWPE Used in Prostheses 581

24.5 Conclusive Remarks and Future Perspectives 583

References. 584

Part VII Dissipation Mechanisms at Finite Separations

25 Casimir Force and Frictional Drag Between Graphene Sheets . . . 591

Aleksandr I. Volokitin and Bo Persson

 25.1 Introduction 591

 25.2 Fluctuations Produce Forces 593

 25.3 Reflection Produces Friction. 600

 25.4 Using Graphene to Detect Quantum Friction 601

 25.5 Conclusion. 605

References. 606

26 Dissipation at Large Separations 609

Marcin Kisiel, Markus Langer, Urs Gysin, Simon Rast, E. Meyer and Dong-Weon Lee

 26.1 Introduction 610

 26.2 Internal Friction of the Cantilever 613

 26.2.1 Thermo-elastic Damping 614

 26.2.2 Bulk and Surface Losses 615

 26.3 Dissipation at Large Separations 616

 26.3.1 Dissipation due to Electromagnetic Interaction 617

 26.3.2 Suppression of Electronic Friction in the Superconducting State 619

 26.3.3 The Noncontact Friction due to Phase Slips of the Charge Density Wave (CDW) in NbSe₂ Sample. 622

 26.4 Summary and Conclusions. 626

References. 626

Part VIII Applications

27 Nanotribology of MEMS/NEMS 631

Satish Achanta and Jean-Pierre Celis

 27.1 MEMS/NEMS Devices, Applications, and Their Reliability Issues 632

27.2 Tribological Problems in MEMS/NEMS 634

27.3 Tribological Evaluation of Materials for MEMS/NEMS 636

 27.3.1 Background on Adhesion, Friction and Wear
 at Nano-/Micro- Scales 636

 27.3.2 Techniques for Tribological Characterization
 of Materials 637

 27.3.3 Tribological Evaluation of Materials 638

27.4 Prospective Materials. 648

27.5 Conclusions 652

References. 652

28 Nanotribology in Automotive Industry. 657

Martin Dienwiebel and Matthias Scherge

28.1 Introduction 657

 28.1.1 Wear and Length Scales 658

28.2 Energetic View of Friction and Wear 659

28.3 The “Third Body”. 660

28.4 Nanowear 662

 28.4.1 Composition of the Near-surface Material 663

 28.4.2 Friction- and Wear-Induced Changes
 of the Surface. 664

 28.4.3 Structural Changes of the Mixed Zone. 664

 28.4.4 Wear Debris. 666

 28.4.5 Atomic-Scale Wear Studies 666

28.5 Conclusions 667

References. 668

29 Adhesion and Friction Contributions to Cell Motility 669

Mario D’Acunto, Serena Danti and Ovidio Salvetti

29.1 Introduction 670

29.2 Cell Motility: A General Overview 671

 29.2.1 Actin Based Motility 672

 29.2.2 Traction Force Microscopy 673

29.3 Mechanotaxis and Scaffold Surfaces 676

 29.3.1 Role of Roughness 680

29.4 Adhesion and Friction Models for Cell Motility 684

 29.4.1 Actin-Based Motility Models 685

 29.4.2 Active Gels Model 691

 29.4.3 Polymerization of Viscoelastic Gel Confined
 in a Channel 693

29.5 Conclusions and Future Perspectives 695

References. 695

Index 699

Contributors

Satish Achanta Department of MTM, Katholieke Universiteit Leuven, Leuven, Belgium

Nicolas Agraït Departamento de Física de la Materia Condensada C-III, Universidad Autónoma de Madrid, Madrid, Spain

Guillaume Anciaux Ecole Polytechnique Fédérale de Lausanne, Lausanne, Switzerland

Itay Barel Department of Chemistry and Biochemistry, University of California, Santa Barbara, USA

Roland Bennewitz INM—Leibniz-Institute for New Materials, Saarbrücken, Germany; Physics Department, Saarland University, Campus D2 2, Saarbrücken, Germany

Oleg M. Braun Institute of Physics, National Academy of Sciences of Ukraine, Kiev, Ukraine

Lorenzo Bruschi CNISM Unitá di Padova, Padova, Italy

Seymour Cahangirov Nano-Bio Spectroscopy Group, Departamento Física de Materiales, Centro de Física de Materiales CSIC-UPV/EHU-MPC and DIPC, Universidad Del País Vasco, San Sebastian, Spain

Rosario Capozza International School for Advanced Studies (SISSA), Via Bonomea 265, Trieste, Italy

Giuseppe Carbone CEMeC Politecnico di Bari, Bari, Italy

Jean-Pierre Celis Department of MTM, Katholieke Universiteit Leuven, Leuven, Belgium

- Salim Ciraci** Department of Physics, Bilkent University, Ankara, Turkey
- Rogério Colaço** Department of BioEngineering and Centro de Química Estrutural, Instituto Superior Técnico, Universidade de Lisboa, Lisbon, Portugal
- Maria Teresa Cuberes** Dpto. Mecánica Aplicada, Universidad de Castilla-La Mancha, Almadén, Spain
- Mario D’Acunto** Istituto di Struttura Della Materia, Consiglio Nazionale Delle Ricerche (ISM-CNR), Roma, Italy; Istituto di Scienza E Tecnologie Dell’Informazione, Consiglio Nazionale Delle Ricerche, ISTI-CNR, Pisa, Italy; NanoICT Laboratory, Area Della Ricerca CNR, Pisa, Italy
- Serena Danti** Department of Surgical, Medical, Molecular Pathology and Emergency Medicine, University of Pisa, Pisa, Italy
- Martin Dienwiebel** Karlsruhe Institute of Technology, Institute for Applied Materials—Reliability of Systems and Components, Microtribology Center μ TC, Karlsruhe, Germany
- Dirk Dietzel** Institute of Applied Physics (IAP), Justus-Liebig-Universität, Gießen, Germany
- Franco Dinelli** Istituto Nazionale di Ottica, INO-CNR, Pisa, Italy
- Leonid Dorogin** Institute of Physics, University of Tartu, Tartu, Estonia
- Carlos Drummond** Centre de Recherche Paul Pascal, CNRS-Université Bordeaux 1, Pessac, France
- Mykhaylo Evstigneev** Faculty of Physics, University of Bielefeld, Bielefeld, Germany
- Joost W. M. Frenken** Kamerlingh Onnes Laboratory, Leiden University, Leiden, The Netherlands
- Enrico Gnecco** Instituto Madrileño de Estudios Avanzados en Nanociencia, IMDEA Nanociencia, Campus Universitario de Cantoblanco, Madrid, Spain
- Urs Gysin** Institute of Physics, University of Basel, Basel, Switzerland
- Haidara Hamidou** Institut de Science des Matériaux de Mulhouse, Mulhouse, France
- Kenichi Hiratsuka** Chiba Institute of Technology, Narashino-shi, Chiba, Japan
- Ilmar Kink** Institute of Physics, University of Tartu, Tartu, Estonia
- Marcin Kisiel** Institute of Physics, University of Basel, Basel, Switzerland
- Markus Langer** Institute of Physics, University of Basel, Basel, Switzerland
- Dong-Weon Lee** MEMS and Nanotechnology Laboratory, Chonnam National University, Gwangju, South Korea

Rünno Lõhmus Institute of Physics, University of Tartu, Tartu, Estonia

Sabine Maier Department of Physics, University of Erlangen-Nürnberg, Erlangen, Germany

Nicola Manini Dipartimento di Fisica, Università degli Studi di Milano, Milano, Italy

Juan J. Mazo Departamento de Física de la Materia Condensada, Instituto de Ciencia de Materiales de Aragón, CSIC-Universidad de Zaragoza, Zaragoza, Spain

Ernst Meyer Institute of Physics, University of Basel, Basel, Switzerland

Giampaolo Mistura CNISM and Dipartimento di Fisica e Astronomia G. Galilei, Università di Padova, Padova, Italy

Jean-Francois Molinari Ecole Polytechnique Fédérale de Lausanne, Lausanne, Switzerland

Karine Mougín Institut de Science des Matériaux de Mulhouse, Mulhouse, France

Martin H. Müser Jülich Supercomputing Centre, Forschungszentrum Jülich, Jülich, Germany; Universität des Saarlandes, Saarbrücken, Germany

Roman Nevshupa IETCC, CSIC, Madrid, Spain

Bo Persson Peter Grünberg Institut, Forschungszentrum Jülich, Jülich, Germany

Carlos Pimentel Departamento de Cristalografía y Mineralogía, Universidad Complutense de Madrid, Instituto de Geociencias (UCM-CSIC), Madrid, Spain

Carlos M. Pina Departamento de Cristalografía y Mineralogía, Universidad Complutense de Madrid, Instituto de Geociencias (UCM-CSIC), Madrid, Spain

Pasqualantonio Pingue NEST, Scuola Normale Superiore and Istituto Nanoscienze—CNR, Pisa, Italy

Boris Polyakov Institute of Solid State Physics, University of Latvia, Riga, Latvia

Srinivasa Babu Ramiseti University of Edinburgh, Edinburgh, UK

Simon Rast Institute of Physics, University of Basel, Basel, Switzerland

Peter Reimann Faculty of Physics, University of Bielefeld, Bielefeld, Germany

Philippe Richetti Centre de Recherche Paul Pascal, CNRS-Université Bordeaux 1, Pessac, France

Juan J. Riquelme Departamento de Física de la Materia Condensada C-III, Universidad Autónoma de Madrid, Madrid, Spain

Gabino Rubio-Bollinger Departamento de Física de la Materia Condensada C-III, Universidad Autónoma de Madrid, Madrid, Spain

Ovidio Salvetti Istituto di Scienza E Tecnologie Dell'Informazione, Consiglio Nazionale Delle Ricerche, ISTI-CNR, Pisa, Italy

Vladimir N. Samoïlov IFF, FZ-Jülich, Jülich, Germany

Matthias Scherge Fraunhofer IWM, Microtribology Center, Pfinztal, Germany

André Schirmeisen Institute of Applied Physics (IAP), Justus-Liebig-Universität, Giessen, Germany

Udo D. Schwarz Department of Mechanical Engineering and Materials Science and Center for Research on Structures and Phenomena (CRISP), Yale University, New Haven, CT, USA

Ion M. Sivebaek Department of Mechanical Engineering, Technical University of Denmark, Lyngby, Denmark

Ugo Tartaglino Pirelli Tires, Milan, Italy

Erio Tosatti CNR-IOM Democritos National Simulation Center, Trieste, Italy; International School for Advanced Studies (SISSA), Trieste, Italy; International Center for Theoretical Physics (ICTP), Trieste, Italy

Michael Urbakh School of Chemistry, Tel Aviv University, Tel Aviv, Israel

Andrea Vanossi CNR-IOM Democritos National Simulation Center, Trieste, Italy; International School for Advanced Studies (SISSA), Trieste, Italy

Sebastian Vieira Departamento de Física de la Materia Condensada C-III, Universidad Autónoma de Madrid, Madrid, Spain

Sergei Vlassov Institute of Physics, University of Tartu, Tartu, Estonia

Aleksandr I. Volokitin Samara State Technical University, Samara, Russia

Chunyan Yang IFF, FZ-Jülich, Jülich, Germany

Part I
Experimental Techniques

Chapter 1

Friction Force Microscopy

Roland Bennewitz

Abstract This chapter introduces Friction Force Microscopy, which is possibly the most important experimental technique in nanotribology. In spite of the apparent simplicity of this technique, a special care is required in the calibration of the force sensors, as discussed in the chapter. We will also present a few key results on the load, material and temperature dependence of friction. The chapter ends with an overview on dynamic measurements of friction, in which the probing tip is oscillated laterally while sliding in contact with the sample surface or even while translating at very close distance from it.

1.1 Introduction

Friction Force Microscopy (FFM) is a sub-field of scanning force microscopy addressing the measurement of lateral forces in small sliding contacts. In line with all scanning probe methods, the basic idea is to exploit the local interactions with a very sharp probe for obtaining microscopic information on surfaces in lateral resolution. In FFM, the apex of a sharp tip is brought into contact with a sample surface, and the lateral forces are recorded while tip and sample slide relative to each other. There are several areas of motivation to study FFM. First, the understanding of friction between sliding surfaces in general is a very complex problem due to multiple points of contact between surfaces and the importance of lubricants and third bodies in the sliding process. By reducing one surface to a single asperity, preparing a well-defined structure of the sample surface, and controlling the normal load on the contact the complexity of friction studies is greatly reduced and basic insights into the relevant processes can be obtained. Furthermore, with the decrease of the size of mechanical devices (MEMS) the friction and adhesion of small contacts becomes a technological issue. Finally, the lateral resolution allows to reveal tribological contrasts caused by material differences on heterogenous surfaces.

R. Bennewitz (✉)
INM–Leibniz Institute for New Materials, Saarbrücken, Germany
e-mail: roland.bennewitz@inm-gmbh.de

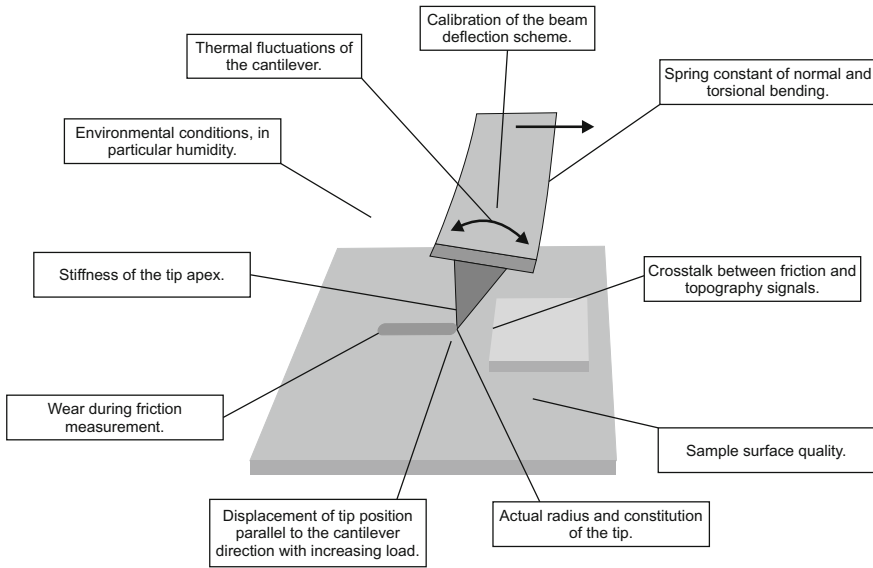


Fig. 1.1 Critical issues in experimental friction force microscopy which are discussed in this chapter

The experimental field of FFM has been pioneered by Mate et al. [1]. The group built a scanning force microscope where the lateral deflection of a tungsten wire could be measured through optical interferometry. When the etched tip of the tungsten wire slid over a graphite surface, lateral forces exhibited a modulation with the atomic periodicity of the graphite lattice. Furthermore, an essentially linear load dependence of the lateral force could be established.

In this chapter we will describe aspects of instrumentation and measurement procedures. In the course of this description, a series of critical issues in FFM will be discussed which are summarized in Fig. 1.1.

1.2 Instrumentation

1.2.1 Force Sensors

The force sensor in the original presentation of FFM by Mate et al. was a tungsten wire [1]. Its deflection was detected by an interferometric scheme where the wire constituted one mirror of the interferometer. A similar concept was later implemented by Hirano et al., who optically detected the deflection of the tungsten wire in a Scanning Tunneling Microscope when scanning the tip in close proximity to the surface [2]. Mate and Hirano report lateral spring constants from 1.5 to 2,500 N/m, depending on the wire thickness and length. Etching the wire to form a tip at its end,

mounting the wire, aligning of the light beam, and determination of the spring constant comprise some experimental difficulties. These difficulties are greatly reduced by the use of dedicated micro-fabricated force sensors. A very sophisticated instrumental approach to the solution of those problems has been realized by Dienwiebel et al. [3]. The group has attached a stiff tungsten wire to a micro-fabricated force sensor made of silicon. The central part of the sensor is a pyramid holding the tip. The position of the pyramid is detected in all three dimensions by means of four optical interferometers directed towards the faces of the pyramid. It is suspended in four symmetric high-aspect ratio legs which serve as springs with isotropic spring constant in both lateral directions and a higher spring constant in normal direction. The symmetric design of the instrument allows for determination of normal and lateral forces acting on the tip with minimal cross talk. An overview over different experimental realizations of FFM is given in Fig. 1.2.

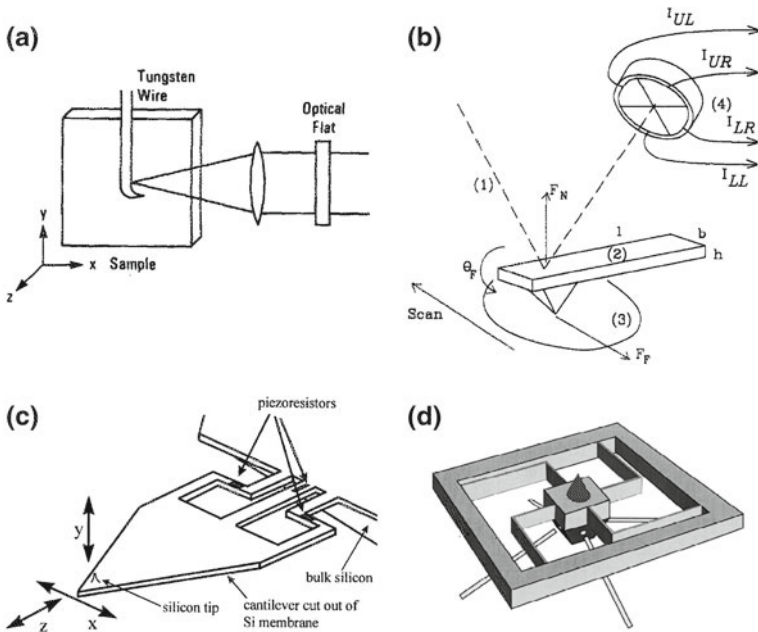


Fig. 1.2 Four design options for Friction Force Microscopy. **a** Concept of the original instrument used by Mate et al. for their pioneering experiments [1] The deflection of a tungsten wire is detected by optical interferometry. The bent end of the wire is etched into a sharp tip. **b** Beam-deflection scheme as devised by Marti et al. [5]. Normal force F_N and friction force F_F cause bending and twisting of the cantilever. The deflection of a reflected light beam is recorded by comparing currents from four sections of a photodiode. **c** Cantilever device for the measurement of lateral forces with piezoresistive detection [8]. Lateral forces acting on the tip cause a difference in stress across the piezoresistors. **d** Micro-fabricated force detector for isotropic measurements of friction forces. The block in the center holds a tungsten tip, pointing upwards in this figure. The position of the block in all three dimensions is recorded by four interferometric distance sensors which are indicated by the four light beams below the devices [9]

The most widely used form of micro-fabricated force sensors for FFM is the micro-fabricated cantilever with integrated tip. The cantilever can be either a rectangular beam or a triangular design based on two beams. The lateral force acting on the tip is detected as torsional deflection of the cantilever. This scheme has been implemented in 1990 by Meyer et al. [4] and Marti et al. [5]. It is interesting to note that the triangular design is more susceptible to deflection by lateral forces than the rectangular beam, contrary to common belief and intuition [6]. However, triangular cantilevers are less prone to the highly unwanted in-plane bending [7].

The deflection of cantilever-type force sensors is usually detected by means of a light beam reflected from the back side of the cantilever at the position of the tip. The reflected light beam is directed towards a position-sensitive photodiode which detects normal and torsional bending of the cantilever as a shift in the position of the light beam in orthogonal directions. Realistically, there is always some cross-talk between the signals for normal and torsional bending. It can be detected by exciting the cantilever to oscillate at the fundamental normal and torsional resonance and measuring the oscillation amplitude in the orthogonal channels. The cross-talk can be minimized by rotation of the position-sensitive photodiode or accounted for in the detection electronics or software. Cross-talk can transfer topographic features into the lateral force signal and create topographic artifacts from friction contrast, the latter even amplified by the feedback circuit acting on the sample height.

Calibration of the beam-deflection scheme is not a simple task, however very important in order to compare FFM results from different sources. Many publications in the past have reported on relative changes in frictional properties, without providing any calibration at all. While such relative changes certainly represent important physical findings, it is nevertheless of utmost importance to provide all experimental information available, often allowing for a rough quantitative estimate of the lateral forces. Lateral forces in FFM can easily range from piconewton to micronewton, spanning a range of very different situations in contact mechanics, and knowing at least the order of magnitude of forces helps to sort the results qualitatively into different regimes.

The calibration comprises two steps. First, the spring constant has to be determined for the force sensor. Note that the beam-deflection scheme actually determines the angular deflection of the cantilever. Nevertheless it has become custom to quantify the force constant in N/m, where the length scale refers to the lateral displacement of the tip apex relative to the unbent cantilever. Second, a relation between the deflection of the cantilever and the voltage readout of the instrument has to be established.

For the determination of the spring constant, several methods have been suggested. The easiest to calculate it from the dimensions of the cantilever. While width and thickness are easily determined by optical or electron microscopy, thickness is better deduced from the cantilever's resonance frequency. Alternatively, the spring constant can be determined from changes in the resonances caused by the addition of masses to the free end of the cantilever. Also, the analysis of a cantilever's resonance structure in air can provide the required quantities. The latter two methods have recently been described and compared by Green et al. [10]. The relation between tip displacement

and voltage readout can be established by trapping the tip in a surface structure and displacing the sample laterally by small distances. For a rough estimate one can also assume that the sensitivity of the position-sensitive photodiode is the same for normal and torsional deflection. Taking into account the geometry of the beam-deflection scheme, the torsional deflection sensitivity can be deduced from the normal deflection sensitivity (See [11] and page 352 of [12]). Since the quantification of the thermal noise driven torsional resonance can be difficult, a combination of thermal noise and beam geometry methods can be useful for the calibration of FFM [13].

A method which provides a direct calibration of the lateral force with respect to the readout voltage is the comparison with a calibrated spring standard. Recent implementations of this approach suggest as calibrated standards optical fibers [14] or micro-fabricated spring-suspended stages with spring constants that can be traced to international standards [15]. Similarly, the lateral stiffness of a magnetically levitated graphite sheet can be used as [16]. A particularly elegant method to calibrate FFM experiments is the analysis of friction loops, i.e. lateral force curves from forward and backward scans, recorded across surfaces with well-defined wedges [11, 17, 18]. Dedicated micro-fabrication design in form of a hammer-shaped cantilever can also help to calibrate the torsional bending [19].

The torsional deflection of a cantilever can in principle be detected also by optical interferometry, provided that the beam diameter is smaller than the cantilever and the point of reflection is shifted off the torsional axis [20]. However, FFM results including normal and lateral force measurements require the differential reading of multiple interferometers [3, 21].

An alternative to the detection of the cantilever bending via the beam-deflection scheme is the implementation of piezoresistive strain sensors into the cantilever. In order to measure both lateral and normal forces acting on the tip in FFM, two such strain sensors need to be realized on one sensor. Chui et al. have created a piezoresistive sensor which decouples the two degrees of freedom by attaching a normal triangular cantilever to a series of vertical ribs sensing lateral forces [22]. Gotszalk et al. have constructed a U-shaped cantilever with one piezoresistive sensor in each arm, allowing for the detection of lateral forces at the tip [23]. While the publications presenting these novel instrumental approaches contain experimental proofs of concept, no further use of piezoresistive sensors in FFM experiments has been reported. This is certainly due to a lack of commercial availability. Furthermore, the signal-to-noise ratio in static force measurements using piezoresistive cantilevers seems not to reach that of optical detection schemes.

1.2.2 Control Over the Contact

The exact knowledge of the atomic configuration in the contact between tip apex and surface is prerequisite for a complete understanding of the results in Friction Force Microscopy. It is the most severe drawback in FFM that this knowledge is not available in most cases. While sample surfaces can often be prepared with atomic

precision and cleanliness, the atomic constitution of the tip apex is usually less controlled. Friction signals vary with tip shape, as has been investigated for steps on graphite [24]. Furthermore, in the course of sliding atoms may be transferred from the tip to the surface or vice versa. Such transfer processes occur even for very gentle contact formation, as shown in experiments combining Scanning Probe Microscopy with a mass spectrometry analysis of the tip apex [25–27]. The transfer of atoms may quite often not only quantitatively but also qualitatively change the lateral forces encountered. Chemical reactions between surface and tip have been found to significantly increase friction between a Pt(111) surface for silicon but not for diamond tips [28]. The occurrence of atomic stick-slip motion can depend on the establishment of a certain degree of structural commensurability between tip and surface in the course of scanning [29, 30]. For atomic stick-slip measurements on graphite surfaces, the role of small graphite flakes attached to the tip has long been discussed and recently confirmed experimentally [1, 31].

The best control over the atomic structure of the tip apex has been achieved for metal tips in vacuum environments. By applying the established procedures of Field Ion Microscopy (FIM), the tip structure can not only be imaged but also conditioned on the atomic scale. Cross et al. have characterized the adhesion between a tungsten tip and a gold surface and proved the conservation of the atomic tip structure by means of FIM [32]. Even with instruments of lower resolution, FIM can at least be used for cleaning procedures and for a determination of the crystalline orientation of the apex cluster [2].

The integrated tips at the end of micro-fabricated silicon cantilevers have a well-defined crystalline orientation, usually pointing with the (100) direction along the tip. However, the tip surface and with it the whole tip apex are at least oxidized and possibly contaminated through packaging, transport, and handling. Furthermore, many tips are sharpened in a oxidation process which introduces large stresses at the apex. While etching in hydrofluoric acid can remove the oxide and for some time passivate silicon surface bonds by hydrogen, a stable formation and reproducible characterization comparable with FIM of metal tips has not yet been reported. Tips integrated into silicon nitride cantilevers are amorphous due to the chemical vapor deposition process and may exhibit an ever more complex structure and chemistry at the tip apex.

One way of overcoming the uncertainty of the tip constitution is to use methods of surface chemistry to functionalize the tip [33]. Specific interactions between molecules attached to the tip and molecules on the surface can be sensed by means of FFM [34]. At the same time, very strong adhesion has been reduced by covering the tip with a passivating layer to allow for lateral force imaging for example on silicon [35]. Numerous studies using this method have been published, mainly concentrating on organic monolayers on tip and surface. A review of the field has been given by Leggett et al. [36]. While most tip functionalization relies on thiol bonding to gold-coated tips, carbon bonding to nanocrystalline diamond tips has also been realized [37]. Schwarz et al. have prepared well-defined tips for FFM by deposition of carbon from residual gas molecules in a Transmission Electron Microscope, keeping control of the tip radius for a quantitative analysis of a contact mechanics

study [38]. Force measurements explicitly aiming at interactions between colloidal particles and a surface have been performed by gluing micrometer-sized spheres of the desired size to the cantilever [39, 40]. As a final note, one should always be aware of the possible occurrence of major tip wear which has been observed to happen in a concerted action of mechanical and chemical polishing [41].

1.3 Measurement Procedures

The standard measurement in FFM is the so-called friction loop: The lateral force acting on the tip is recorded for a certain distance of scanning in the direction perpendicular to the long cantilever axis and for the reverse direction. The area in the loop represents the dissipated energy, and the area divided by twice the distance is the mean lateral force. It is always very instructive to record the topography signal of forward and backward scan at the same time, as differences will reveal cross-talk between normal and torsional bending of the cantilever.

Whenever lateral forces are measured as a function of some experimental parameter, the influence of that parameter on adhesion should be studied simultaneously. In order to interpret the experimental results in terms of contact sizes versus dissipation channels the knowledge of adhesion is essential. An excellent example is the jump in lateral forces observed on a C_{60} crystal when cooling to the orientational order-disorder phase transition, which was fully explained by a change in adhesion [42]. For experiments carried out in ambient environment, the dominant contribution to adhesion are usually capillary forces which dependent greatly on the humidity and on the hydrophobicity of the surface [43]. The humidity dependence of FFM results itself can depend again on the temperature [44–46]. Consequently, an enclosure of FFM experiments for humidity control greatly enhances the reproducibility of results.

1.3.1 Friction as a Function of Load

One of the central experiments in tribology is the quantification of friction, i.e. the change of lateral force with increasing normal load on the sliding contact. One of the questions to be addressed is whether the relation between lateral and normal force is linear for FFM experiments, i.e. whether Amontons' law extends to the nanometer scale [47]. The number of FFM studies reporting lateral force as a function of load is very large, and the overall physical picture is multifaceted, to express it in a positive way. A collection of results is shown in Fig. 1.3. From a procedural point of view it is extremely important to measure the lateral forces for the full range of small normal forces until the tip jumps out of contact, usually at a negative normal force. In this way the adhesion in the system can be categorized and even maps of adhesion can be produced from friction versus load experiments [48]. Furthermore,